

Numerical Calculation of the Heat Transfer Characteristics of Fuel Cladding with Dirt at Low Coolant Speed

S.H. Yin, X.Y. Zhang¹, A.Q. Liu

School of Electric power, South China University of Technology
Guangzhou 510640, China
scuttotti@163.com; zxy1119@scut.edu.cn; 814032919@qq.com

ABSTRACT

Research of the flow and heat transfer characteristic of fuel cladding with dirt at low coolant speed is very important for cooling of the fuel assembly in LOCA. Therefore, a heated fuel rod with spacer grids and covered with dirt on the surface has been taken for investigation. The one-dimensional flowing and heat transfer model of the coolant and fuel cladding has been developed, time steady and transient simulation have been completed. Effect of dirt that blocking the flowing passage on heat transfer deterioration of fuel cladding has been studied, the influence of the dirt thickness, heat conductivity and coolant speed have been investigated. As the verification, the computed results of a 1/4 section fuel rod in this work has been compared with simulated results from the CFD analysis, the comparison shows satisfied agreement with the maximum relative deviation less than 2%. From the full study of coolant flowing and heat transfer for the 1/4 section fuel rod, we have following three findings. Firstly, dirt deposition outside the fuel rod leads to a higher wall temperature than a clean fuel rod, the increase magnitude of temperature grows up gradually while the dirt thickness increase, but grows down rapidly while the thermal conductivity of the dirt increase. Secondly, speed of the coolant has great influence on cooling of the fuel rod, a very small low coolant velocity would lead to heat transfer deterioration which caused the cladding temperature increasing greatly. Thirdly, the spacer grids has effect of enhancing cooling of the fuel rod, an obvious decrease of cladding temperature would appear in the grids position.

KEYWORDS

fuel cladding; dirt; heat transfer characteristics; low coolant speed

1. INTRODUCTION

After occurrence of LOCA in a nuclear power plant, the emergency core cooling system (ECCS) and containment spray system (CSS) would run for a long time to ensure a continuous core cooling and maintaining long-term containment of pressure and temperature within the range of acceptable. After refueling tank reaches the low water level, the ECCS and CSS system will automatically switch to the recirculation mode, taking water from the containment pit. In some cases, the fragment from pipeline breakage would flow with coolant in the core, or sprayed liquid would migrate into the containment pit filter in other cases, causing block of the filter. Integrity of the fuel rod may be endangered when the flowing channel is blocked due to accumulation of large fragments, which causes the coolant flow blockage accident in some fuel assemblies. This accident may cause blocked fuel assemblies lacking enough cooling, make fuel clad temperature rising rapidly and result in strong evaporation of coolant. In that condition, the release of radioactive material to the coolant is very possible, and the safety of the fuel cladding is highly threatened. Therefore, study the thermalhydraulic characteristics and safety

¹Corresponding author: X.Y. Zhang, zxy1119@scut.edu.cn

¹This work is co-sponsored by the National Natural Science Foundation of China (51376065, 51176052), Guangdong Key Scientific Project (2013B010405004), Guangdong Province Key Laboratory of Efficient and Clean Energy Utilization (2013A061401005), South China University of technology; Key Laboratory of Efficient and Clean Energy Utilization of Guangdong Higher Education Institutes (KLB10004).

characteristics of the fuel rod assemblies in condition of dirt deposition are very important to the safe operation of PWR nuclear power plants.

Much study on flow and heat transfer of a fuel rod has been carried out in past decades. M.Schikorr[1] had used the “Rehme” equation to calculate the pressure drop of the bundle with a spacer grid. Podowski[2] had used two-phase flow and heat transfer dimensional physical model to predict the critical heat flux of fuel rods. Alajbegovic[3] had used two-phase CFD model to analysis the mechanism of critical heat flux on forced convective sub-cooled boiling. Chen[4] had made numerical analysis for thermal-hydraulic characteristics of 17×17 fuel assemblies in losing external cooling. Yang[5] had made a three-dimensional analysis of flow and heat transfer characteristics in supercritical PWR coolant channels. Sreenivas Jayanti[6] had developed a three-zone model to calculate the heat transfer characteristics of the fuel rods when evaporated phenomenon occurs. LuoLei[7] had used a one-dimensional model to calculate the radial heat transfer of fuel elements with a uniform heat flux, temperature of the fuel element and its surrounding coolant had been studied. Liu Yizhe[8] had used the CFX to study the coolant flowing data in fuel assemblies of China Experimental Fast Reactor. Liu tian cai[9] had used the Relap5 code to calculate the core power, pressure, flow and temperature changes of China Advanced Research Reactor power when suffering blocking flow accident. Song Lei[10] had used CFD code to make a transient analysis of fuel assembly in the core entrance part, in 95% blocking accident and fully blocking accident. Shi xiaobo[11] had established the theoretical simulation model of fully blocking accident in fast reactor fuel assembly, to study the accident sequence on a single fuel assembly in fully blocking accident with normal core power condition.

In summary, there is little study on thermal hydraulic characteristics of the fuel rod cladding considering the low coolant speed and dirt deposition at present. This paper will focus on coolant blockage and heat transfer characteristic of fuel cladding with dirt at low coolant speed. The 1D homogeneous fluid model will be established to study the transient and steady state temperature distribution of cladding surface. Influence of the dirt thick, dirt heat conductivity and coolant flowing speed on fuel cladding temperature will be investigated. The CFD simulation will also be made to verify the theoretical model and computed results.

2. Geometry and condition parameters

In this paper, an entire length fuel rod will be taken into consideration. There are six wide grids and three narrow grids along the entire rod height, and height of narrow grid is half of the wide grid. The shape of grid cross section is square. It's assumed that the rear 1/3height part of the fuel cladding is covered with the dirt. Thickness of dirt is uniform along the fuel rod. The grid is tightly bounded outside the fuel rod cladding. Considering the geometric symmetry, only 1/4 fuel rods section and the fluid channel will be taken for study. Figure 1 provides a schematic drawing of fuel bundle. A simplified cross section geometry of fuel rod covered with dirt and flowing channel is shown in Figure 2, where “A1” is the coolant flowing zone, “A2” is the dirt layer, “A” is the cladding layer. In location of spacer grid, Figure 3 provides the structure of cross section, where an equal thick layer of spaced grid is embedded between the cladding and dirt. The main geometry parameter of fuel rod of CPR1000 has been taken in this study. The cladding inner diameter is 8.36mm, outer diameter is 9.5mm, and the space between adjacent rods is 12.6mm. Six types of dirt thickness have been taken for investigation: 0、 δ 、 2δ 、 3δ 、 4δ and 6δ , where δ is 0.225mm.

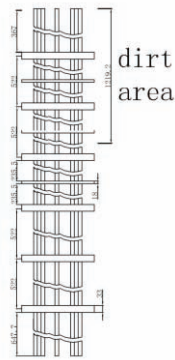


Fig1. Fuel assembly frame diagram

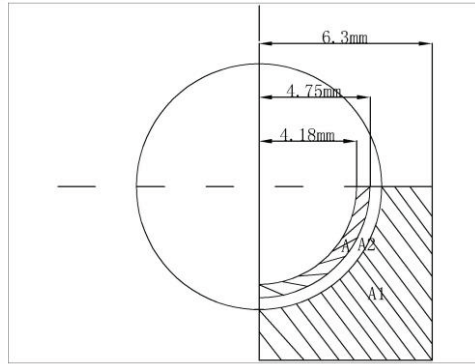


Fig 2. Fuel assembly cross section

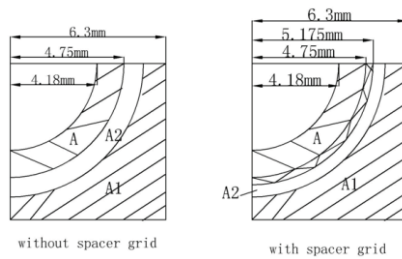


Fig3. Spacer grid geometry

In choosing condition parameters, we consider that after LOCA accident, the reactor will shut down and also the primary pump will shut down. Long-time stage cooling of the core depending on the natural circulation of coolant, so the entrance coolant speed into the core is very low in this condition. The pressure is close to the pressure of reactor containment and fluid temperature is about temperature of hot shut down. In above consideration, the following condition parameters are chosen in computation of this work. Fluid temperature at flowing entrance outside the fuel rod is 120°C, which is also the initial fluid temperature for transient analysis. The heat flux on fuel rod cladding is 30000w/m², and the working pressure of fluid is assumed 4bar. To study effect of flowing speed, six entrance fluid speeds will be used for investigation, that is u_0 , $2u_0$, $3u_0$, $4u_0$, $5u_0$, and $6u_0$, where u_0 is 0.01m/s. To study influence of dirt conductivity, four values of conductivity have been used in computation, that is λ , 2λ , 3λ and 4λ , where λ is 0.17w/(m•K).

3. Mathematical model

To study the flowing and heat transfer characteristic between fluid and cladding on the upward vertical flowing channel, the one dimensional flowing conversation equations has been established including the fluid mass, energy and momentum equation. Solving the equations will give the enthalpy, velocity, temperature and pressure of coolant. Temperature of fuel rod cladding will be determined by flow patterns and calculation of heat transfer.

3.1. Conservation equation of fluid

Using the homogeneous model to calculate the fluid parameter along the height of flowing channel, the following conservation equations can be written out.

$$2\rho A \frac{\partial H}{\partial \tau} + m \frac{\partial H}{\partial z} = q_l \quad (1)$$

$$\frac{\partial(\rho A)}{\partial \tau} + \frac{\partial(GA)}{\partial z} = 0 \quad (2)$$

$$\frac{\partial(GA)}{\partial \tau} + \frac{\partial(vG^2A)}{\partial z} = -A \frac{\partial p}{\partial z} - \frac{fvAG|G|}{2De} - \rho gA \quad (3)$$

In solving above equations, the scheme of timing backward difference and spacing upwind difference has been adopted. For transient analysis, a pressure correction iteration scheme is adopted for each time step. Firstly, assuming fluid pressure of new time step equals that of previous time step and computes all required thermophysical properties like ρ , c_p , ν . Then solve the energy equations to calculate the coolant enthalpy along the height of rod. And solve the mass equations to calculate coolant velocity along the height. Finally solve the conservation equations to correct the coolant pressure on the new time step, that means end of one iteration. Then using the corrected pressure to recalculate the coolant thermophysical properties, and start next iteration. The iteration will not stop until the calculated out pressure at the channel ends equals to the initial set value.

3.2 Calculation of pressure loss

Friction pressure loss along the whole rod length has been considered in this work. For friction pressure loss for single phase flow and two phase flow, the following two formulas are adopted to computed the friction coefficients respectively,

$$f = \frac{64}{\text{Re}}, \quad f = \frac{4 \times 0.079 \rho_f}{\text{Re}^{0.25} \rho_v} \left(1 + x \left(\frac{\rho_v}{\rho_g} - 1\right)\right) \left(1 + x \left(\frac{\mu_v}{\mu_l} - 1\right)\right)^{-0.25} \quad (4)$$

And for form loss of spacer grids, the proposed formula of Rehme has been used as,

$$\Delta p_{gd} = K_d \phi^2 \frac{\rho V^2}{2} \quad (5)$$

3.3 Flowing patterns transition

In this study, the coolant flows vertically upward along the fuel rod height at a low speed. Flowing patterns will begin with a single-phase region in the entrance, then changes to sub-cooled boiling after heated by the fuel rod, and changes to saturated boiling region. In cases of very small coolant mass flow, even excessive boiling region or single-phase steam region may arise at end part of the flowing channel. As the heat transfer coefficient in different flowing pattern regions varies widely, we must find the transition points between different flow patterns, including the onset of nucleate boiling (ONB), the bubble detachment surface (FDB), saturated boiling point (SAT), the critical heat flux (CHF) and dry-out point (DRY).

Onset of nucleate boiling (ONB) is the transition point from the single phase to two-phase flowing. Heat transfer characteristics of that point are not only single phase, but also nucleate boiling heat transfer. So the Jens-Lottes[12] formula is used to calculate the position of ONB. As for FDB, the Saha-zuber[13] model will be used. For the saturated boiling starting point, this work adopts the position where fluid's enthalpy equals the specific enthalpy of saturated liquid. The CHF relationship of low pressure and low flow conditions proposed by Satish G.Kandikar[14] is used here to calculate the critical heat flux point (CHF).

$$\left(\frac{q_{CHF}}{h_{fg}}\right)^2 \left(\frac{D_h}{\rho_V}\right) = a_1 \sigma (1 + \cos \theta_R) + a_2 \frac{G^2 D_h (1-x)}{\rho_m} + a_3 \frac{\mu_l G (1-x)}{\rho_l} \quad (6)$$

The above formula is proposed for conditions of $G=23\sim 53000\text{Kg}/(\text{m}^2\text{s})$, $P=0.047\sim 1.55\text{Mpa}$, hydraulic diameter is ranging from 0.127mm to 3.36mm. The range of mass flow and pressure in this work is adapted to above equation. While the hydraulic diameter of this work is ranging from 3.44mm to 11.77mm, that's a little higher than the proposed range. After comparing results of CHF with Eq.6 in this work with the 2006 CHF look-up table[17], it's found that correlation of S.G. Kandikar is suitable for condition of this work.

The dry-out point is assumed to come when the void rate $x_g>0.99$.

3.4 Calculation of heat transfer coefficient

Flowing is single phase from the entrance to the FDB point. Because the coolant speed is very low with $Re<1000$, flowing pattern in entrance part is in a laminar flow state. In the other side, as heat flux on the fuel rod is relatively high, natural convection must be taken into consideration. So heat transfer correlations of Mihai Aliyev[12] is used in this paper to calculate the heat transfer coefficient in single phase region that is,

$$Nu = 0.15 \left(\frac{GD_e}{\mu_f} \right)^{0.33} \left(\frac{C_p \mu}{k} \right)_f^{0.43} \left(\frac{Pr_f}{Pr_w} \right)^{0.25} \left(\frac{D_e g \rho_f \alpha_v \Delta T}{\mu_f^2} \right)^{0.1} \quad (7)$$

Flowing pattern from FDB point and SAT is sub-cooled nucleate boiling region. The extended Chen formula of sub-cooled nucleate boiling is used in this region, which takes both single-phase forced convection and natural convection into consideration[15].

$$h^2 = h_l^2 + h_{nb}^2 \quad (8)$$

Flowing pattern between SAT and CHF point is saturated nucleate boiling. There are two kinds of heat transfer mechanisms in this region, one is nucleate boiling, another is forced convection. Roles of the two mechanisms can be interacted. The saturated nucleate boiling formula of Chen is used in this work to calculate the heat transfer coefficient in this region.

$$h = h_l F(X_{tt}) + h_{nb} S(Re_{tp}) \quad (9)$$

As for heat transfer between CHF and dry-out point, the formula of Li Hongbo[16] is used,

$$h_{FB,DNB} = 0.0232 \left(\frac{T_{sat} - T_{f,in}}{T_w - T_{sat}} \right)^{\frac{1}{5}} \frac{k_l}{D_h} Re^{\frac{1}{2}} Pr_f \quad (10)$$

The proposed parameter ranges for equation (10) is mass flux being $47.53\sim 1500\text{kg}/(\text{m}^2\text{s})$, pressure being $0.3\sim 10\text{Mpa}$, the hydraulic diameter being $8\sim 12\text{mm}$, the inlet sub-cooled temperature being $0.65\sim 70^\circ\text{C}$, and heat flux being $32.91\sim 1443.58\text{kw}/\text{m}^2$, which is applicable to this work.

After liquid phase coolant is over heated to dry out, flowing in the channel becomes single phase steam. Also, the Dittus-Boelter formula is used to calculate the heat transfer coefficient in the region.

3.5 Calculation of fuel cladding temperature

Based on above calculation of fluid temperature field and the convective heat transfer coefficient, now the Newton heat transfer formula is used to calculate the fuel rod wall temperature.

$$T_w(i) = \frac{Q}{h(i)A(i)} + T_f(i) \quad (11)$$

Wall temperature in dirt layer and cladding layer is assumed only varying with clad radius, which can be computed with one-dimensional heat conduction equation in cylindrical coordinates. In computing wall temperature with differencing equation of Eq.12, the k_w use conductivity of dirt and steel in dirt layer and cladding layer, respectively.

$$C_w \rho_w \frac{\partial T_w}{\partial \tau} = \frac{1}{r} \frac{\partial}{\partial r} \left(k_w r \frac{\partial T_w}{\partial r} \right) + q_v \quad (12)$$

4. Simulation with CFD code

For verification of above mathematical model and results, one case of the problem has been taken for investigation with CFX. In CFD analysis, the geometrical model of 1/4 fuel rods and coolant channel was established using UG software, and the grids mesh was made with ICEM. The divided mesh is structured. The number of nodes is 2207520. Figure 4 shows the calculation mesh on the cross section, figure 5 shows the mesh quality. The entrance velocity of coolant is $2u_0$, temperature is 120°C . Heating rate at the internal side of cladding wall is 30000w/m^2 . At end of the channel, the bounding type is set as opening with pressure of 4bar. Choose phase change model as two phase flow model, and select k-e model and simple calculation method, residual convergence is 0.0001. In solving of CFD, the type of interphase transfer takes particle model, the mass transfer type takes thermal phase change, the two phase model takes RPI model.

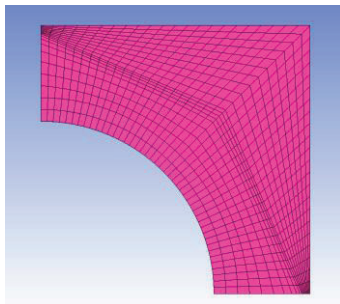


Fig4.Fluid domain mesh division result

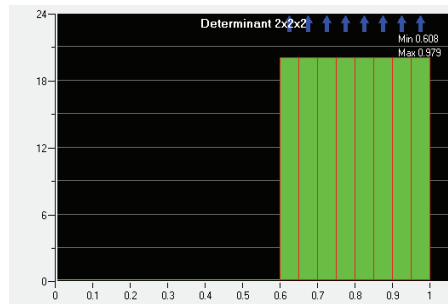


Fig5.Mesh quality

5. Calculation results and analysis

5.1 Comparing results with CFD simulation

To verify the established mathematical theory and computing results, compare the simulation result from the CFD code with the calculating results in condition of flow velocity being $2u_0$, dirt thickness being 6δ , and dirt conductivity coefficient being λ . The comparison of coolant temperature is shown in figure 6. It's shown that the two set of results are in good agreement, with a small deviation less than 2%. One can also find that coolant temperature rise rapidly after entering the flowing channel and gets saturation point closely after the entrance. The temperature rising trend of CFD simulation is not so steep like that of computing results. The reason is that mesh size along the rod height in numerical calculation is much big than CFD simulation. Increasing of fluid temperature in entrance part is so rapid, requires a more fine mesh to give a better precision. The comparison of cladding temperature from CFD simulation and numerical calculation is shown in figure 7. Also, good agreement will be find between the two sets of results.

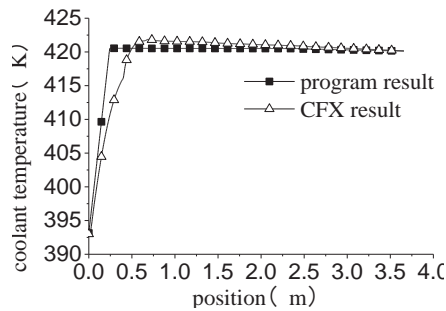


Fig6. Verification of coolant temperature result

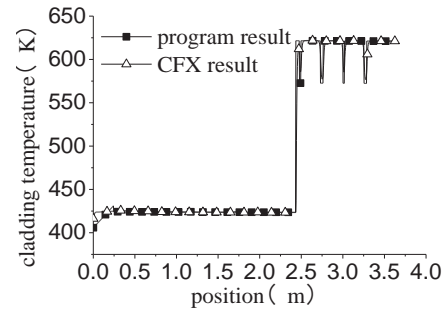


Fig7. Verification of cladding temperature result

5.2 Detailed results of coolant and fuel cladding in low mass flow

5.2.1 Transient and steady state calculation under low mass flow conditions

The steady and transient analysis has been made in condition of inlet velocity being $2u_0$, dirt thickness being 6δ and dirt conductivity being λ . The coolant temperature change along the rod height is shown in figure 8. We can find that in position before 0.25m, the coolant temperature rises with the increasing height. When coolant temperature reaches the saturation point, it will keep essentially unchanged in the rear length. Figure 9 shows the coolant temperature along the rod height at several time steps. One can find that the coolant temperature increases from the initial time to 25 seconds. After the initial 25 seconds, coolant temperature rises to the saturated temperature and maintained at that temperature at all the later time steps.

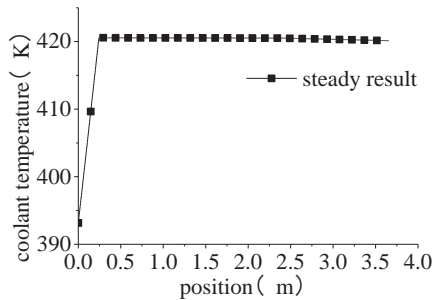


Fig 8. Steady calculation of coolant temperature

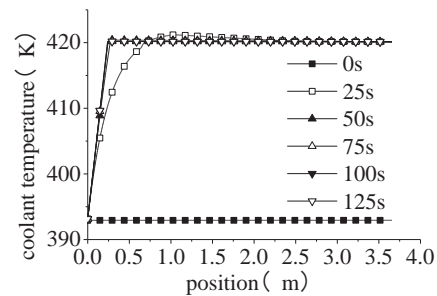


Fig9. Transient calculation of coolant temperature

Figure 10 shows the steady-state calculation results of coolant pressure. As can be seen from this figure, the flowing pattern is single liquid phase and coolant density is very high in entrance part of the flowing channel outside, so the friction loss of pressure is quite strong, that makes the coolant pressure dropped quickly in entrance part. After the entrance part, the coolant pressure drops slower with the increasing axial position, as two phase flowing pattern arises and the coolant density is much small than single liquid phase. At positions after 2.5m, the pressure drop rate increase a bit, as dirt on the fuel rod narrows the flowing area and speeds up the coolant flowing, makes pressure drop increasing then. Figure 11 shows the calculated coolant pressure under transient computation. It's shown that the pressure drop at initial time is highest, being 32000Pa, which will decrease at later times with decreasing density in flowing pattern transition. Comparing with Fig.10, we find that coolant pressure will come to stable after 75s, with a constant pressure drop to be 3000Pa.

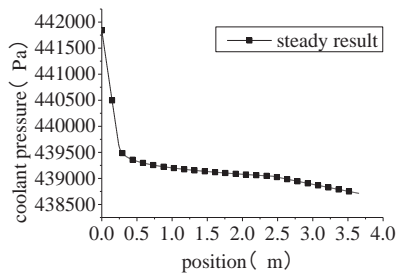


Fig10. Steady calculation of coolant pressure

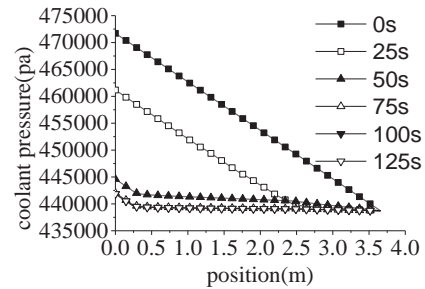


Fig11. Transient calculation of coolant pressure

Figure 12 shows the calculation results of temperature on outer surface of cladding under steady state. It can be seen that in the entrance part, the temperature on outer surface of the rod cladding increases with the height. Closely after the entrance, the coolant temperature rise to the saturation point of the working pressure, both the coolant and cladding temperature keeps constant in a rather long length. The cladding temperature keeps constant towards 2/3 of rod height, where dirt layer appears. There one can find an increase of 200K in cladding temperature, as a large heat conduction resistance exists between the coolant and the cladding. At positions of spacer grid, the cladding temperature is lower than non grid position, as the thermal conductivity of grid is higher than that of dirt. Figure 13 shows the transient results of cladding temperature. As can be seen, the cladding temperature rises quickly from the initial value and reaches a steady state from the initial time to 25s. The reason is the thin thickness, high conductivity and low heat capacity of the cladding material.

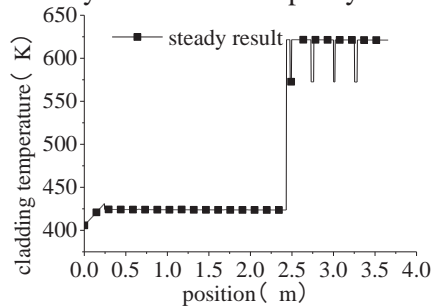


Fig12. Steady calculation of cladding temperature

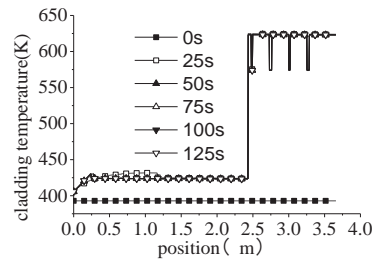


Fig13. Transient result of cladding temperature

5.2.2. Influence of dirt thickness

In order to analyze influence of dirt thickness on cladding temperature, we use six dirt thicknesses for computation. The inlet coolant velocity is $2u_0$, and dirt thermal conductivity is λ , these parameters are constant in all the six computations.

Figure 14 shows variation of coolant temperature with thickness of dirt. It can be seen that when the dirt is thicker, the increasing rate of coolant temperature in entrance part of flowing channel is higher, also means the sub cooling length is shorter. Because fluid velocity and pressure drop would rise for thicker dirt, which would enhance the heat transfer in flowing channel and shorten the sub cooling length.

Figure 15 shows variation of integrated heat transfer coefficient with thickness of dirt. The integrated heat transfer coefficient includes heat transfer coefficient of convection of fluid and conduction of dirt. It can be seen from the figure that the heat transfer coefficient will steep rise to very high after entering the flowing channel, which is corresponding to transition of flow pattern from sub cooling boiling to saturation boiling. For the thicker dirt, the transition position will get closer to the entrance. In the outlet

part of flowing channel, a steep drop of heat transfer coefficient can be found for the five dirt thickness being $2\delta\sim6\delta$, which means serious cooling deterioration coming up caused by the dirt. But for dirt with thickness being δ , there isn't difference in heat transfer coefficient between the clean part and dirt covered part.

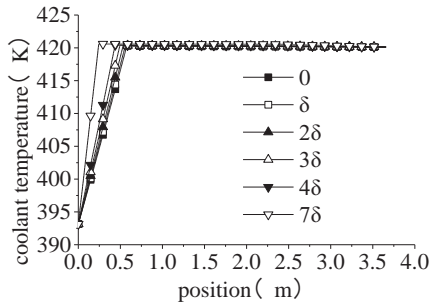


Fig14. Calculation of coolant temperature

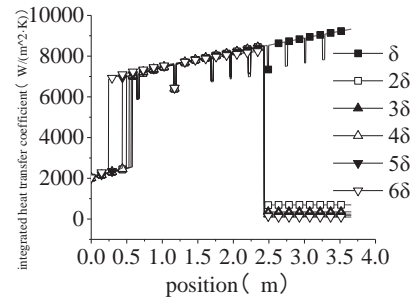


Fig15. Calculation of heat transfer coefficient

Figure 16 shows coolant pressure in flowing channel with dirt of 6 thicknesses. One can find that variation of dirt thickness in $\delta\sim6\delta$ does not change pressure drop along the whole channel length, but the drop gradient in outlet part will be larger when thickness is 6δ . Figure 17 shows variation of fuel cladding temperature with the dirt thickness. As can be seen from the figure, cladding temperature in clean part of cladding is not affected by dirt thickness. In dirt covered part, cladding temperature increase greatly, the increase is higher for thicker dirt. The cladding temperature covered with dirt thickness being 6δ is 200K higher than that with thickness being δ .

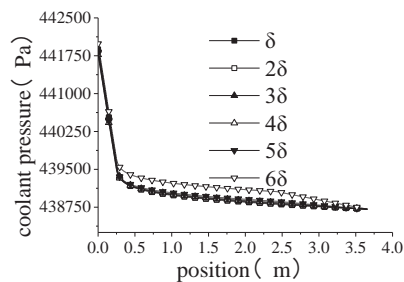


Fig16. Calculation of coolant pressure

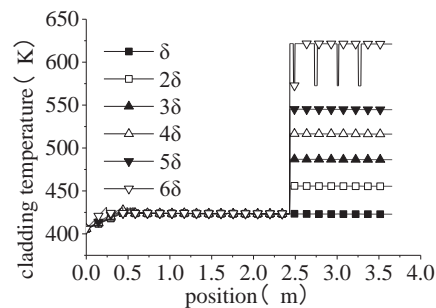


Fig17. Calculation of cladding temperature

5.2.3. Influence of dirt conductivity

In order to analyze influence of dirt conductivity on cladding temperature, four conductivities of the dirt, $\lambda\sim4\lambda$, have been taken for calculation in this work. The inlet coolant velocity is $2u_0$, dirt thickness is 6δ in this analysis. Figure 18 shows results of integrated heat transfer coefficient for the with the dirt conductivity. It can be seen that in dirt covered cladding, the heat transfer coefficient drops greatly compared to the clean cladding. The heat transfer coefficient decreases with the decreasing of thermal conductivity. When the dirt conductivity is lower, decrease range of heat transfer coefficient is higher.

Figure 19 shows effect of dirt conductivity on cladding temperature. It can be seen that the changing dirt conductivity doesn't affect cladding temperature of the clean part. In dirt covered cladding, dirt conductivity shows noticeable influence on cladding temperature, which grows much higher for smaller. The dirt covered cladding temperature decreases from 630K to 470K when dirt conductivity increases from λ to 2λ .

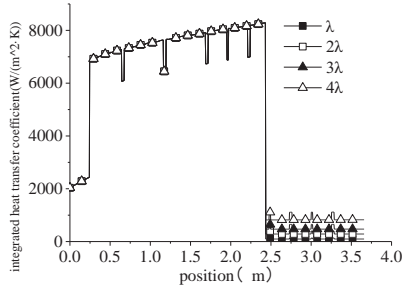


Fig 18. Calculation of heat transfer coefficient

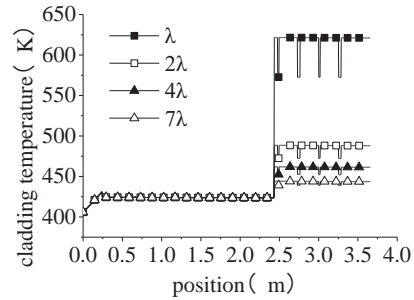


Fig19. Calculation of cladding temperature

5.2.3. Influence of coolant speed

In order to analyze influence of inlet coolant speed on cladding temperature, six inlet coolant speeds in $u_0 \sim 6u_0$ have been used in this work. Dirt thickness is 6δ and conductivity is λ in this computation. Figure 20 shows coolant temperature along the rod height for the 6 inlet coolant velocities. It can be seen from the figure that the coolant temperature almost keeps constant along the whole rod height for inlet coolant speed in $2u_0 \sim 6u_0$. But when inlet coolant speed is u_0 , coolant temperature rises linearly in the dirt covered part of flowing channel. As dry out pattern occurs in that case and the steam temperature keeps rising with heated from the fuel rod. Figure 21 shows change of heat transfer coefficient with inlet coolant velocity. One can see that position of enhancing heat transfer moves forward along the rod height in entrance part with increasing inlet coolant velocity, caused by increasing length of single phase flowing pattern. In the dirt covered cladding, heat transfer coefficient increases by speeding up of coolant for inlet coolant velocity being $2u_0 \sim 6u_0$. Drop of heat transfer coefficient and cooling deterioration on dirt covered cladding only occurs when inlet coolant velocity is u_0 .

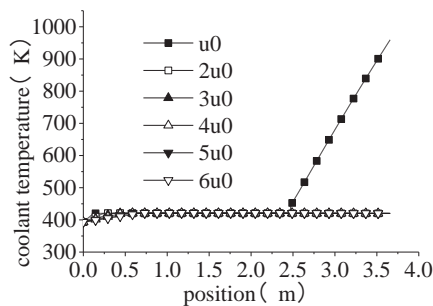


Fig20. Calculation of coolant temperature

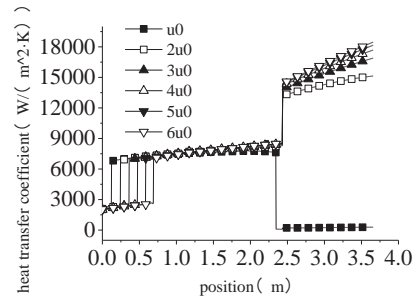


Fig 21. Calculation of heat transfer coefficient

Figure 22 shows cladding temperature for different inlet coolant velocity. It can be seen that cladding temperature almost keeps constant when velocity is $2u_0 \sim 6u_0$. But when velocity is u_0 , cladding temperature rises linearly along the dirt covered height, caused by steep drop of heat transfer coefficient. The maximum cladding temperature appears at outlet of fuel rod, being 1200K. That is very dangerous for integrity of fuel cladding. Figure 23 shows coolant pressure for different inlet coolant velocity, one can find that pressure drop of the flowing channel grows up rapidly with increase of inlet coolant velocity.

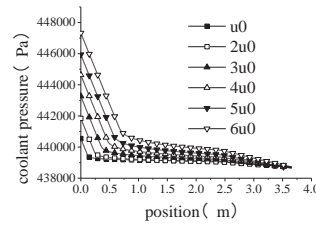
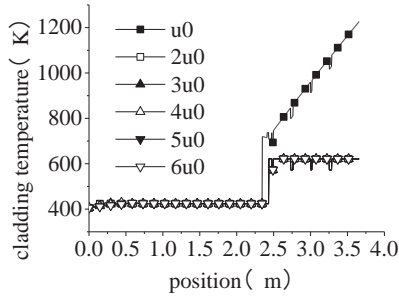


Fig22.Cladding temperature in variable velocity Fig23.Coolant pressure in variable velocity

6. Conclusion

Heat transfer and cladding temperature in condition of low coolant velocity and with dirt covered on the cladding has been studied in this work. A one-dimensional homogenous model of flowing has been established to compute the time steady and transient coolant flowing data along the rod height, heat transfer coefficient and cladding temperature has been computed. One verification case has been taken for calculation, and results have been compared with simulation of CFD code. Effects of dirt thickness, heat conductivity and coolant speed have been investigated.

The study shows that the coolant temperature increases with time in the initial 25 seconds, which will be maintained at saturated temperature after that time when inlet velocity is $2u_0$, dirt thickness is 6δ and dirt conductivity is λ . The cladding temperature is about 10K higher than coolant in clean part of cladding, but is about 220K higher than coolant in dirt covered part. Increasing dirt thickness from δ to 2δ ~ 6δ may cause cooling deterioration and make cladding temperature covered with dirt 40~200K higher than clean cladding. Increasing dirt conductivity and coolant velocity could eliminate cooling deterioration of the fuel cladding by the dirt.

NOMENCLATURE

variable name	variable meaning	variable unit
H	Enthalpy	KJ/(mol*k)
ρ	Density	Kg/ m ³
A	Flow area	m ²
m	Mass flow	Kg/s
h	Heat transfer coefficient	w/(m ² *k)
q _l	Liner power density	w/m
t	Temperature	°C
z	Location	m
τ	Time	s
G	Mass flow density	Kg/(m ² *s)
V	Velocity	m/s
P	Pressure	pa
f	Coefficient of friction	
v	Specific volume	m ³ /Kg
D_e	Equivalent diameter	m
g	Gravitational acceleration	m/s ²
q _{CHF}	Critical Heat Flux	W/m ²
h _{fg}	Latent heat of vaporization	J/(Kg*k)
D_h	Equivalent diameter	m
ρ_v	Saturated vapor density	Kg/m ³
σ	Surface tension	N/m

θ_R	Receding contact angle	deg
x	void fraction	
ρ_m	Average density	Kg/m ³
a1	Constant value:1.03e-4	
a2	Constant value:5.78e-5	
a3	Constant value:0.783	
Nu	Nusselt number	
μ_f	Fluid viscosity	Pa*s
Cp	Specific heat capacity at constant pressure	
i	Time node	
n	Location Node	
T _f	Coolant temperature	K
T _w	Wall temperature of tfuel rods	K
q _{CHF}	Critical Heat Flux	W/m ²
h _{fg}	Latent heat of vaporization	J/(Kg*k)
α	Volume expansion coefficient	1/K
F	The proportion of forced convective heat convection in the total proportion of convection heat transfer	
K _d	Form loss coefficient of spacer grid	
ϕ	Ratio of front area of spacer grid and flowing channel	
S	Nucleate boiling inhibitory factor	
ρ_g	Saturated vapor density	Kg/m ³
ρ_l	Saturated liquid density	Kg/m ³
μ_G	Saturated vapor dynamic viscosity	Pa*s
μ_L	Saturated liquid viscosity	Pa*s
T _{sat}	Saturation temperature corresponding to the pressure	K
k _L	Thermal conductivity of saturated liquid corresponding to the pressure	W/(m*k)
Pr _g	Saturated steam Prandtl number	
x	void fraction	
X _{tt}	$X_{tt} = \left(\frac{1-x}{x}\right)^{0.75} \left(\frac{\rho_g}{\rho_l}\right)^{0.5} \left(\frac{\mu_l}{\mu_g}\right)^{0.1}$	

SUBSCRIPTS

w	Wall
sat	Saturated condition
in	At the inlet section
f	Fluid
l	Liquid
g	Void
DNB	Departure from Nucleate Boiling

REFERENCES

- [1] M.Schikorr and E.Bubelis and L.Mansani and K.Litfin,"Proposal for pressure drop prediction for a fuel bundle with grid spacers using Rehme pressure drop correlations,"*Nuclear Engineering and Design*. **240**(7),pp.1830-1842(2010).
- [2] Podowski,"CFD prediction of flow and Phase distribution in fuel assemblies with spacers,"*Nuclear Engineering and Design*, **177**(1),pp.215-228(1997).

- [3] Alajbegovic, "An analysis of phase distribution and turbulence in dispersed particle/liquid flows," *Chemical engineering communications*. **174**(1), pp.154-167(1999).
- [4] S.R.Chen and W.C.Lin and Y.M.Ferng and C.C.Chieng and B.S.Pei, "CFD simulating the transient thermal-hydraulic characteristics in a 17×17 bundle for a spent fuel pool under the loss of external cooling system accident," *Annals of Nuclear Energy*. **73**, pp.272-280(2014)
- [5] Xingbo.yang and G.H.Su and WenxiTian and Jiayun Wang and SuizhengQiu, "Numerical study on flow and heat transfer characteristics in the rod bundle channels under super critical pressure condition," *Annals of Nuclear Energy*. **37**(12), pp.1723-1734(2010).
- [6] Sreenivas Jayanti and Michel Valette. "Calculation of dry out and post dry out heat transfer in rod bundles using a three field model," *International Journal of Heat and Mass Transfer*. **48**(9), pp.1825-1839(2005).
- [7] LUO Lei and CHEN Wen zhen and CHEN Zhiyun and ZHU Qian. "Numerical simulation of thermal hydrodynamic of single reactor fuel rod," *Journal of naval university of engineering*. **23**(1), pp.63-72(2012).
- [8] LIU YI-zhe and YU Hong, "Thermal-Hydraulic Analysis of Fuel Subassemblies for Sodium-Cooled Fast Reactor," *Atomic Energy Science and Technology*. **42**(2), pp.128-134(2008)
- [9] Liu Tian-cai and JIN Hua-jin and YUAN Lu-zheng. "Flow Blockage Accident Analysis for China Advanced Research Reactor," *Nuclear Power Engineering*. **27**(5), pp.32-44(2006).
- [10] Song Lei and Guo Yun and ZengHeyi. "Numerical Analysis on Transient Flow and Temperature Field During Inlet Flow Blockage Accidents of Plate-type Fuel Assembly", *Nuclear Power Engineering*. **35**(3), pp.6-10(2013).
- [11] SHI Xiao-bo and LUO Rui and WANG Zhou. "Modeling of Accident Scenario Caused by Total Blockage of Single Subassembly in a Fast Reactor and its Validation", *Nuclear Power Engineering*. **27**(1), pp.37-42(2006).
- [12] HAO Lao-mi. *Nuclear reactor thermal hydraulics*. Atomic Energy Press, pp.36-58(2010), First Edition, Beijing, In Chinese.
- [13] YU Ping-an and ZHU Rui-an and YU Zhen-Wan, SHEN Xiu-zhong. *Nuclear Reactor Thermal Analysis*, Shanghai Jiao tong University Press, pp.36-43(1979), in Chinese.
- [14] Satish G. Kandlikar. "A Scale Analysis Based Theoretical Force Balance Model of Critical Heat Flux (CHF) During Saturated Flow Boiling in microchannels and Minichannels," *Journal of Heat Transfer*, **132**(8), pp.1-13(2010).
- [15] REN Ze-pei. *Heat transfer*. Higher Education Press, pp.243-246(1998), in Chinese.
- [16] LI Hong-bo and CHEN Bing-de and ZHAO Hua and XIONG Wan-yu. "Numerical model of post-DNB film boiling heat transfer," *Nuclear Science and Engineering*, **31**(2), pp.146-153(2011).
- [17] Groeneveld D C, Shan J Q, Vasić A Z, et al. The 2006 CHF look-up table[J]. *Nuclear Engineering and Design*, **237**(15): 1909-1922(2007).